Using a Stationary Compact Array of Acoustic Sensors to Estimate the Motion Parameters of Sources

Ildar R. Urazghildiiev and David E. Hannay

***Abstract*—Compact arrays of acoustic sensors can provide bearing measurements of detected sounds. An important application for compact arrays is estimating the motion parameters of sources. This work considers the problem of bearings-only estimating of the positions and heading angles of vessels in the presence of bearing and speed measurement errors. Statistical simulations are used to evaluate the dependence of bearing estimation accuracy on the duration of the observation interval and the variance of speed errors. Plots of range and heading estimation errors obtained for 171 vessel passes with known positions are presented. Test results demonstrate that the accuracy of the estimating range depends strongly on speed error variance.**

***Index Terms*—Compact array, estimation errors, maximum likelihood (ML) estimator, target motion analysis.**

I. Introduction

PASSIVE acoustic vessel localizing and tracking plays an important role in port security applications and, more generally, in monitoring coastal and offshore vessel activities. This approach can provide vessel presence and distribution information at locations where other tracking methods such as RADAR or automatic identification system (AIS) are not effective. Passive acoustic monitoring (PAM) approaches can be used, for example, to monitor vessel activities in marine protected areas and conservation areas. The basic requirements of vessel tracking systems are the ability to identify vessels within a surveillance area, and to estimate their headings, speeds, and positions.

Traditionally, large arrays of omnidirectional synchronized acoustic sensors are used in PAM systems (see [1] and references therein). Large arrays with a distance between sensors of hundreds of meters or longer make it possible to locate and track underwater sources using time difference of arrival (TDOA) measurements. An example of a large array consisting of 11 omnidirectional sensors with the distance between elements of 700 . . . 920 m and a maximum array size of 24 382 m is presented in [1]. Large arrays could potentially provide sufficiently accurate position estimates of the sources located close to the array [1]; however, their sheer size makes them difficult to use when near real-time performance is needed. Also, it is difficult to synchronize omnidirectional sensors over long deployment periods. Using stationary compact arrays of synchronized sensors could ease these disadvantages.

Compact arrays having the distance between sensors from 50 m [2] to 0.5–2 m [3]–[9] can measure the azimuth and elevation angle of detected sounds using TDOA-based or beamforming-based localization techniques, and they have near real-time capability when connected to a data processing station. Various heuristic techniques [2]–[8] have been implemented using stationary compact arrays to locate and track vessels and marine mammals. The reported techniques could address specific needs, but they are not guaranteed to be statistically optimal and their accuracy is often not tested in real-world scenarios.

Theoretically, compact arrays can measure vessel ranges directly from the elevation angles of their sounds and knowing the water depth. This direct method of range measurement generally provides acceptable accuracy for ranges comparable to the water depth near the array. In shallow water areas, the maximum range available for direct measurements is limited and may be insufficient for many practical applications. Therefore, this work is focused on the position estimation problem with a shallow water application only using bearing (or azimuth) measurements. The possibility of direct measurements of vessel ranges is not considered.

The problem of estimating positions and heading angles of sources from bearing measurements is known as the bearing-only target motion analysis (BO-TMA) problem (see e.g., [10]–[21] and references therein). The main difficulty in implementing known BO-TMA techniques is that they require a moving observer, which is difficult to implement for long-term PAM applications.

The problems of motion parameter estimation of aircrafts and ground vehicles using a stationary compact array are considered in [22], [23]. The terrestrial application of compact arrays presented in these works differ from the underwater application considered here in several ways; sound propagation effects are different in ocean environments, sensor to target range intervals are different, and target speeds differ substantially. In particular, the speed of ground vessels is comparable with the speed of sound in air, such that target positions at times of emitting sound and receiving the same sound by the array can differ significantly. This so-called retardation effect is used in [22] to estimate the unknown speed of vehicle. The solution proposed in [23] assumes that the sensor can directly measure the source coordinates in 3-D coordinate systems. Since all mentioned conditions do not hold when estimating motion parameters of

Manuscript received April 11, 2017; revised September 14, 2017; accepted November 6, 2017. Date of publication November 29, 2017; date of current version October 11, 2018. *(Corresponding author: Ildar R. Urazghildiiev.)*

Associate Editor: Z.-H. Michalopoulou.

I. R. Urazghildiiev is with JASCO Applied Sciences (USA), Inc., Anchorage, AK 99501 USA (e-mail: ildar.urazghildiiev@jasco.com).

D. E. Hannay is with JASCO Applied Sciences (Canada), Ltd., Victoria, BC V8Z 7X8, Canada (e-mail: david.hannay@jasco.com).

Digital Object Identifier 10.1109/JOE.2017.2772984

vessels, the results presented in [22], [23] are not directly applicable to the underwater system considered here.

Another important problem not addressed by the existing literature is how to estimate motion parameters when bearing errors are correlated. As shown in [9], bearing errors observed in underwater systems can be correlated because of various unpredictable factors that affect the propagation of sound in water. Because correlated errors can increase estimation errors, corresponding statistically optimal estimators should be designed accordingly and their performance should be evaluated.

Finally, estimation accuracy reported in the previous literature was obtained using statistical simulations [10]–[21], which do not account for all factors that affect the estimation accuracy. Therefore, the performance of the estimators in real-world scenarios needs to be tested.

The main difficulty with implementing known BO-TMA techniques with stationary arrays is that the position estimates are unobservable from the bearing measurements if the speed of sources is unknown [10]–[14]. However, the fact that speed cannot be measured directly does not necessarily mean that there is no speed information available. For example, the distribution of vessel speeds can be obtained from historic vessel AIS data near the array location. The approximate speed of sources can be identified based on the distribution of speeds of similar sources. In many cases, additional speed information can be obtained directly from acoustic measurements of the source being monitored. For example, vessel shaft rate can often be extracted from the acoustic data using envelope modulation methods [24]. Speed errors do not affect heading estimation accuracy but they do affect range estimation accuracy. The range estimation accuracy can still be acceptable in the presence of speed errors, and stationary compact arrays can be an alternative to large arrays of synchronized hydrophones for many applications.

This work considers the problem of estimating the positions and heading angles of sources, using bearing-only measurements from a stationary compact array. We assume that bearing errors are represented as a correlated Gaussian random process with known or estimated statistical characteristics. We also assume that the speed of sources is known approximately. Thus, the position estimates are observable from bearing measurements, but additional position estimation errors occur due to speed uncertainty. The goal of this work is to evaluate the influence of various factors on the accuracy of position and heading estimates. These factors include the duration of correlation interval and variance of bearing errors, the duration of the source observation interval, and the variance of speed errors. The performance of the maximum likelihood (ML) estimator is evaluated using Cramér–Rao bounds (CRB), statistical simulations, and *in situ* tests. The *in situ* tests were conducted using a stationary compact tetrahedral array of hydrophones from JASCO Applied Sciences, Inc., Victoria, BC, Canada, deployed on the Victoria Experimental Network Under the Sea (VENUS) cabled ocean observatory operated by Ocean Networks Canada (ONC) in the Salish Sea, BC, Canada. The main contributions of this work are the closed-form representations for the ML estimator, for estimation errors, and for the CRB, as well as test results representing the estimation accuracy in real-world scenarios.

Section II considers a data model and problem formulation. Section III presents the closed-form representations of the ML estimator. Representations for estimation errors are derived in Section IV. Section V presents the results of simulations and *in situ* tests.

II. Data Model and Problem Formulation

We assume that vessel engines, drivetrain, and propellers are the dominant sources of vessel noise and the difference in position of these components is much smaller than the distance between them and the array. Therefore, in this work vessels are presented as point sources, and the source position is specified by the average position of the noise generating components.

Locating and tracking sources is performed within an area specified in a 2-D Cartesian coordinate system. Axes *X* and *Y* are placed in a horizontal plane, and axis *Y* was oriented to true North. At time t, the position of the source is described by the vector

$$\boldsymbol{r}\left(t\right)=\boldsymbol{r}\left(t_0\right)+v_0\boldsymbol{e}\left(\gamma_0\right)\left(t-t_0\right)=\begin{bmatrix}x\left(t\right)\\ y\left(t\right)\end{bmatrix}\in R^2,\qquad t\in U_t \tag{1}$$

where v_0 is the source's speed; γ_0 is the heading angle; the vector $\boldsymbol{e}(\gamma_0)=[\sin\gamma_0,\cos\gamma_0]^T$ describes the travel direction; $U_t=\{t:t\in[t_0,t_0+T]\}$ is the observation interval; and t_0 and T are start time and the duration of the observation interval, respectively.

We assume that the parameters $x(t_0)=x_0$, $y(t_0)=y_0$, and γ_0 were unknown, such that the parameters to be estimated are defined as the vector

$$\boldsymbol{\theta}_0=\left[x_0,y_0,\gamma_0\right]^T\in R^3 \tag{2}$$

where symbol "*T*" denotes a transpose. The start time t_0 was chosen to specify the vector $\boldsymbol{\theta}_0$ for convenience only. The source position can be estimated for any time $t\in U_t$ by substituting (2) and corresponding value of speed into (1).

A compact array located at the center of the coordinate system estimated the source's bearings at discrete time instances. In this work, we do not make any restrictions on the method of estimating bearings. An example of TDOA-based ML estimator is given in [9], but other algorithms are also applicable. It is assumed that the bearing estimates provided by the array are

$$\hat{\alpha}\left(t\right)=\alpha\left(t,\boldsymbol{\theta}_0\right)+\varepsilon\left(t\right),t\in U_t \tag{3}$$

where

$$\alpha\left(t,\boldsymbol{\theta}_0\right)=\tan^{-1}\frac{x\left(t\right)}{y\left(t\right)} \tag{4}$$

is the true bearing, and $\varepsilon(t)$ is the bearing estimation error.

The true bearing can also be represented as

$$\alpha\left(t,\boldsymbol{\theta}_0\right)=\tan^{-1}\frac{k_v x\left(t\right)}{k_v y\left(t\right)} \tag{5}$$

where $k_v>0$ is a scalar. From (5) it follows that the bearing estimates (3) correspond to an arbitrary trajectory $\boldsymbol{r}(t,v)=k_v\boldsymbol{r}(t_0)+ve(\gamma_0)(t-t_0)$, such that the vector $\boldsymbol{\theta}_0$ is

unobservable from (5)

$$\alpha\left(t,\boldsymbol{\theta}_0\right)=\alpha\left(t,\boldsymbol{\theta}\left(v\right)\right),\qquad v\neq v_0 \tag{6}$$

where $\boldsymbol{\theta}(v)=[k_v x_0, k_v y_0, \gamma_0]^T$ and $k_v = v/v_0$.

To overcome the observability problem, we assume that the unknown speed of a source belongs to a certain region, $v_0 \in [v_{\min},\ v_{\max}]$, such that the mean value $\bar{v}=E\{v_0\}$ and variance σ_v^2 of speeds of all possible sources is known. Provided that $v=\bar{v}$, the vector $\boldsymbol{\theta}(v)$ becomes observable from (3) because there is an unambiguous estimate of $\boldsymbol{\theta}(v)$. However, if $v\neq v_0$, the error

$$\Delta_r=\left\|\boldsymbol{r}\left(t_0,v\right)-\boldsymbol{r}\left(t_0,v_0\right)\right\|>0 \tag{7}$$

of estimating the coordinates x_0 and y_0 occurs, where the symbol $\|\cdot\|$ denotes vector norm.

The vector $\boldsymbol{\theta}_0$ estimation errors also occur due to bearing errors, $\varepsilon(t)$. In published works on BO-TMA problems, bearing [10]–[21], TDOA [22], and position [23] estimation errors are modeled as uncorrelated Gaussian variables, which significantly simplifies the design and analysis of optimal estimators. However, bearing errors provided by an underwater compact array in real-world scenarios can be correlated [9]. This means that the uncorrelated Gaussian process model is inadequate for representing bearing errors. Therefore, the efficiency of the ML estimators should be evaluated for the case of correlated bearing errors.

In this work, we assume that the bearing error $\varepsilon(t)$ is described by a more general Gaussian ergodic correlated process with zero mean, $E\{\varepsilon(t)\}=0$, and known or previously estimated autocorrelation function $C(t,\tau)=C(\tau)=\sigma_\alpha^2\rho(\tau)$, $\rho(0)=1, 0\leq|\rho(\tau)|\leq 1$, where σ_α^2 is the variance and $\rho(\tau)$ is the normalized autocorrelation function. In practice, the parameters $\rho(\tau)$ and σ_α^2 can be an approximated using direct bearing measurements of sources with known coordinates.

The problems considered in this work are formulated as follows.

1) To obtain the closed form representations for the ML estimator of the vector $\boldsymbol{\theta}_0$ (2) and for the corresponding estimation errors.
2) To evaluate the influence of factors such as the duration of correlation interval and the form of correlation matrix of bearing errors, the duration of the observation interval, and the variance of speed errors, on the accuracy of the ML estimates of the vector $\boldsymbol{\theta}_0$.

III. ML Estimator and Variances of the Parameter Estimates

Since a finite number of K bearing measurements is obtained over the observation interval U_t, the bearings (3) can be represented in vector form

$$\hat{\boldsymbol{\alpha}}=\boldsymbol{\alpha}\left(\boldsymbol{\theta}\right)+\boldsymbol{\varepsilon}\ \in R^K \tag{8}$$

where $\hat{\boldsymbol{\alpha}}=[\hat{\alpha}(t_1),\hat{\alpha}(t_2),\ldots,\hat{\alpha}(t_K)]^T$; $\boldsymbol{\alpha}(\boldsymbol{\theta})=[\alpha(t_1,\boldsymbol{\theta}),\alpha(t_2,\boldsymbol{\theta}),\ldots,\alpha(t_K,\boldsymbol{\theta})]^T$; and $\boldsymbol{\varepsilon}=[\varepsilon(t_1),\varepsilon(t_2),\ldots,\varepsilon(t_K)]^T$. With these assumptions, the random vector $\hat{\boldsymbol{\alpha}}$ has a Gaussian distribution with mean $\boldsymbol{\alpha}(\boldsymbol{\theta})$ and a covariance matrix $\boldsymbol{C}=E\{\boldsymbol{\varepsilon}\boldsymbol{\varepsilon}^T\}\in R^{K\times K}$. The logarithmic likelihood function of the vector $\hat{\boldsymbol{\alpha}}$ is

$$lnW\left(\hat{\boldsymbol{\alpha}}|\boldsymbol{\theta}\right)=c-\frac{1}{2}\left(\hat{\boldsymbol{\alpha}}-\boldsymbol{\alpha}\left(\boldsymbol{\theta}\right)\right)^T\boldsymbol{C}^{-1}\left(\hat{\boldsymbol{\alpha}}-\boldsymbol{\alpha}\left(\boldsymbol{\theta}\right)\right) \tag{9}$$

where c is a scalar that does not depend on $\hat{\boldsymbol{\alpha}}$.

From (9), the ML estimate of vector $\boldsymbol{\theta}$ obtained for the speed v is

$$\hat{\boldsymbol{\theta}}=\hat{\boldsymbol{\theta}}\left(v\right)=\left\{\hat{x}_0\left(v\right),\hat{y}_0\left(v\right),\hat{\gamma}_0\right\}=arg\max_{x,y,\gamma}lnW\left(\hat{\boldsymbol{\alpha}}|\boldsymbol{\theta}\right). \tag{10}$$

Correspondingly, the estimate of the source position at any time $t\in U_t$ can be found by substituting the ML estimate of vector $\boldsymbol{\theta}$ (10) into (1)

$$\hat{\boldsymbol{r}}\left(t\right)=\boldsymbol{r}\left(t,\hat{\boldsymbol{\theta}}\left(v\right)\right)=\hat{\boldsymbol{r}}\left(t_0\right)+v\boldsymbol{e}\left(\hat{\gamma}_0\right)\left(t-t_0\right),\qquad t\in U_t. \tag{11}$$

In practice, the estimate (10) can be calculated by using a grid search algorithm that maximizes (9) in 3-D space over the parameters $x,\ \ y$, and γ. The practical implementation of the ML estimator (10) also requires appropriate approximation of the matrix $\boldsymbol{C}$ providing its invertibility.

Choosing the right model for the covariance matrix $\boldsymbol{C}$ is important because it must be nonsingular in order to determine the inverse matrix $\boldsymbol{C}^{-1}$. This matrix must sufficiently approximate the true covariance matrix to maximize the estimation accuracy. The autocorrelation function of bearing errors, $C(\tau)$, can be approximated by various functions. To find the appropriate model for the covariance matrix, we checked sin*c* function

$$C\left(\tau\right)=\sigma_\alpha^2\frac{\sin\left(\tau/\tau_\alpha\right)}{\tau/\tau_\alpha} \tag{12}$$

linear function

$$C\left(\tau\right)=\begin{cases}\sigma_\alpha^2\left(1-\tau/\tau_\alpha\right),\tau<\tau_\alpha\\ 0,\tau\geq\tau_\alpha\end{cases} \tag{13}$$

and exponential function

$$C\left(\tau\right)=\sigma_\alpha^2\exp\left\{-\left(\frac{\tau}{0.5\tau_\alpha}\right)^2\right\}. \tag{14}$$

Here τ_α is the model parameter specifying the duration of the correlation interval.

The matrix $[\boldsymbol{C}]_{i,j}=C(\tau_j)-C(\tau_i)$ composed from the autocorrelation functions (12) and (14) for $\tau_\alpha<T$ and for large dimensions $K>100$ is badly scaled and close to singular. Using linear approximation (13), the covariance matrix provided a singularity property. This matrix was used to compute the ML estimates (10).

The ML estimate of the heading angle is unconditional in the sense that it does not depend on the value of speed

$$\hat{\gamma}_0\left(v\right)=\hat{\gamma}_0\left(v_0\right)=\gamma_0+\delta_v \tag{15}$$

where δ_v is the heading estimation error occurring due to bearing errors. The ML estimates of positions are conditional and

depend on the speed v

$$\hat{x}_0(v) = k_v x_0 + \delta_x \tag{16a}$$

$$\hat{y}_0(v) = k_v y_0 + \delta_y \tag{16b}$$

where $k_v = v/v_0$ is a scalar and δ_x, δ_y are the errors caused by bearing errors.

As follows from (15) and (16), the heading and position estimation errors observed when using the speed value v are

$$\Delta_\gamma(v) = \Delta_\gamma = \hat{\gamma}_0 - \gamma_0 = \delta_\gamma \tag{17a}$$

$$\Delta_x(v) = \hat{x}_0(v) - x_0 = x_0(k_v - 1) + \delta_x \tag{17b}$$

$$\Delta_y(v) = \hat{y}_0(v) - y_0 = y_0(k_v - 1) + \delta_y. \tag{17c}$$

Assuming that $E\{\varepsilon(t)\} = 0$ and $E\{\delta_\gamma\} = E\{\delta_x\} = E\{\delta_y\} = 0$, the mean value of the estimation errors (17) are

$$E\{\Delta_\gamma\} = E\{\hat{\gamma}_0 - \gamma_0\} = 0 \tag{18a}$$

$$E\{\Delta_x(v)\} = E\{\hat{x}_0(v) - x_0\} = x_0\left(\bar{k}_v - 1\right) \tag{18b}$$

$$E\{\Delta_y(v)\} = E\{\hat{y}_0(v) - y_0\} = y_0\left(\bar{k}_v - 1\right) \tag{18c}$$

where $\bar{k}_v = E\{k_v\} = E\{v/v_0\}$.

From (18) it follows that the position estimates have bias if speed errors exist. However, if $v = \bar{v} = E\{v_0\}$, the mean value of k_v is close to unity, $\bar{k}_v = E\{\bar{v}/v_0\} \approx 1$, such that the bias can be negligibly small

$$E\{\Delta_x(\bar{v})\} = E\{\Delta_x\} \approx 0, E\{\Delta_y(\bar{v})\} = E\{\Delta_y\} \approx 0. \tag{19}$$

Hereafter, the dependence of the errors $\Delta_x(v)$ and $\Delta_y(v)$ on the value of speed v is omitted. The variance of the estimates obtained for $v = \bar{v}$ are

$$\sigma_\gamma^2 = E\left\{\left(\Delta_\gamma - E\{\Delta_\gamma\}\right)^2\right\} = E\left\{\Delta_\gamma^2\right\} = \sigma_{\gamma\varepsilon}^2 \tag{20a}$$

$$\sigma_x^2(\bar{v}) = E\left\{\left(\Delta_x - E\{\Delta_x\}\right)^2\right\} \approx E\left\{\Delta_x^2\right\} = x_0^2\sigma_k^2(\bar{v}) + \sigma_{x\varepsilon}^2 \tag{20b}$$

$$\sigma_y^2(\bar{v}) = E\left\{\left(\Delta_y - E\{\Delta_y\}\right)^2\right\} \approx E\left\{\Delta_y^2\right\} = y_0^2\sigma_k^2(\bar{v}) + \sigma_{y\varepsilon}^2 \tag{20c}$$

where

$$\sigma_{\gamma\varepsilon}^2 = E\left\{\delta_\gamma^2\right\}, \quad \sigma_{x\varepsilon}^2 = E\left\{\delta_x^2\right\}, \quad \sigma_{y\varepsilon}^2 = E\left\{\delta_y^2\right\} \tag{21}$$

are the variances of the heading and position estimation errors that occur when bearing errors are present, and

$$\sigma_k^2(\bar{v}) = E\left\{\left(\bar{v}/v_0 - 1\right)^2\right\} \tag{22}$$

is the variance of the value $(\bar{v}/v_0 - 1)$. Note that the speed of source v_0 is the random variable in (18)–(22).

When bearing errors are Gaussian variables, the variances (20) are limited by the CRB that correspond to the case of a known source speed. The CRB are computed from the Fisher information matrix (FIM) defined for the vector $\boldsymbol{\theta}_0$ (2) as

$$\boldsymbol{F}(\boldsymbol{\theta}_0) = -E\left\{\frac{\partial^2 \ln W(\hat{\boldsymbol{\alpha}}|\boldsymbol{\theta}_0)}{\partial\boldsymbol{\theta}_0\partial\boldsymbol{\theta}_0^T}\right\} = \begin{bmatrix} F_{1,1} & F_{1,2} & F_{1,3} \\ F_{2,1} & F_{2,2} & F_{2,3} \\ F_{3,1} & F_{3,2} & F_{3,3} \end{bmatrix}. \tag{23}$$

Taking into account (9), the elements of FIM are given by [13] and [25]

$$F_{i,j} = [\boldsymbol{F}(\boldsymbol{\theta}_0)]_{i,j} = \left[\frac{\partial\boldsymbol{\alpha}(\boldsymbol{\theta}_0)}{\partial\theta_i}\right]^T \boldsymbol{C}^{-1}\left[\frac{\partial\boldsymbol{\alpha}(\boldsymbol{\theta}_0)}{\partial\theta_j}\right], \quad i,j = 1\ldots3 \tag{24}$$

where

$$\frac{\partial\boldsymbol{\alpha}(\boldsymbol{\theta}_0)}{\partial\theta_i} = \left[\frac{\partial\alpha(t_1,\boldsymbol{\theta}_0)}{\partial\theta_i}, \frac{\partial\alpha(t_2,\boldsymbol{\theta}_0)}{\partial\theta_i}, \ldots, \frac{\partial\alpha(t_K,\boldsymbol{\theta}_0)}{\partial\theta_i}\right]^T \tag{25}$$

is the $K \times 1$ vector of partial derivatives of the true bearings (5). Partial derivatives from the elements of vector $\boldsymbol{\alpha}(\boldsymbol{\theta})$ over the parameters x, y, and γ are

$$\frac{\partial\alpha(t_k,\boldsymbol{\theta}_0)}{\partial x} = \frac{y(t_k)}{d^2(t_k)} \tag{26a}$$

$$\frac{\partial\alpha(t_k,\boldsymbol{\theta}_0)}{\partial y} = \frac{x(t_k)}{d^2(t_k)} \tag{26b}$$

$$\frac{\partial\alpha(t_k,\boldsymbol{\theta}_0)}{\partial\gamma} = v(t_k - t_0)\frac{y(t_k)\cos\gamma + x(t_k)\sin\gamma}{d^2(t_k)} \tag{26c}$$

where

$$d^2(t_k) = x^2(t_k) + y^2(t_k). \tag{27}$$

Since the position estimates are independent of the heading estimates, the CRB for the estimates of the vector $\boldsymbol{\theta}_0$ that corresponds to the case of a known speed of source are given by [13]

$$\sigma_{x\varepsilon}^2 \geq \left[\boldsymbol{F}_{xy}^{-1}(\boldsymbol{\theta}_0)\right]_{1,1} \tag{28a}$$

$$\sigma_{y\varepsilon}^2 \geq \left[\boldsymbol{F}_{xy}^{-1}(\boldsymbol{\theta}_0)\right]_{2,2} \tag{28b}$$

$$\sigma_{\gamma\varepsilon}^2 \geq \left[\boldsymbol{F}^{-1}(\boldsymbol{\theta}_0)\right]_{3,3} \tag{28c}$$

where

$$F_{xy}(\boldsymbol{\theta}_0) = \begin{bmatrix} F_{1,1} & F_{1,2} \\ F_{2,1} & F_{2,2} \end{bmatrix}. \tag{29}$$

Substituting (22)–(29) into (20) gives the variance of the ML parameter estimates (10) computed for the mean value of speeds $v = \bar{v}$ of all sources of interest.

IV. Test Results

Root mean square errors (RMSE) obtained at the closest point of approach (CPA) were used to evaluate the performance of the ML estimator (10). The goal of the tests was to evaluate the influence of various parameters on the RMSE of the range and heading estimates. The tested parameters included the correlation interval τ of bearing errors; the observation interval T; standard deviation (STD) σ_v of the speed of sources; and the

CPA distance, d_{CPA}. The CPA distance and the CPA time were found from (1) as

$$d_{\mathrm{CPA}} = \min_t \|\boldsymbol{r}(t)\| = \|\boldsymbol{r}(t_{\mathrm{CPA}})\| \tag{30a}$$

$$t_{\mathrm{CPA}} = \arg\min_t \|\boldsymbol{r}(t)\|. \tag{30b}$$

The CPA distance and time estimates were obtained from the position estimates (11) using (30).

We assume that a compact array providing azimuth and elevation angle measurements is deployed in shallow water, such that the direct estimation of vessel ranges using the elevation angles is not possible and azimuths only are used to estimate vessel motion parameters in a 2-D space. Correspondingly, horizontal ranges are considered in this section.

A. Simulations

Statistical simulations were conducted for a single vessel traveling with a constant speed of $v_0 = 7$ m/s, the heading angle $\gamma_0 = 45°$, and different distances to the CPA point $d_{\mathrm{CPA}} = 500 \ldots 2000$ m. For each simulation point, the corresponding RMSE were computed using $L = 1000$ runs. In each run, bearing errors were simulated as a random Gaussian process with $\sigma_\alpha = 2°$ and a correlation interval $\tau_\alpha = 0 \ldots 150$ s. Correlated bearing errors were generated using uncorrelated Gaussian process passing through the sixth-order Butterworth lowpass filter, which provided the necessary correlation interval. We assumed that the parameters σ_α and τ_α were known. In practice, these parameters can be measured using vessels with known GPS coordinates as in [9]. The RMSE of range and heading estimates were defined as

$$\mathrm{RMSE}_r = \sqrt{(L)^{-1} \sum_{l=1}^{L} \left(\hat{d}_l - d_{\mathrm{CPA}}\right)^2}$$

$$\mathrm{RMSE}_\gamma = \sqrt{(L)^{-1} \sum_{l=1}^{L} \left(\hat{\gamma}_l - \gamma_0\right)^2}$$

where $\hat{d}_l = \min_t \|\hat{\boldsymbol{r}}(t)\| = \|\hat{\boldsymbol{r}}(\hat{t}_{\mathrm{CPA}})\|$ and $\hat{\gamma}_l$ are the CPA range and heading estimates obtained in the lth simulation run, respectively.

The first simulation scenario evaluated the dependence of RMSE of range and heading estimates on the CPA distance d_{CPA} and on the correlation interval of bearing errors τ_α. We assumed that the source speed was known. The ML estimates were computed using both a diagonal covariance matrix $\boldsymbol{C} = \sigma_\alpha^2 \boldsymbol{I}$ that corresponded to uncorrelated bearing errors, and a matrix with nonzero off-diagonal elements that corresponded to correlated errors and which were composed using the linear approximation (13). The observation time was $T = 200$ s. The simulation results are shown in Fig. 1.

In the second scenario, RMSE of range and heading estimates as functions of CPA distance d_{CPA} and observation time T were computed for correlation interval of bearing errors $\tau_\alpha = 150$ s and the known source speed. The simulation results are shown in Fig. 2.

In the third scenario, the influence of speed errors on the RMSE of range and heading estimates was evaluated. The plots

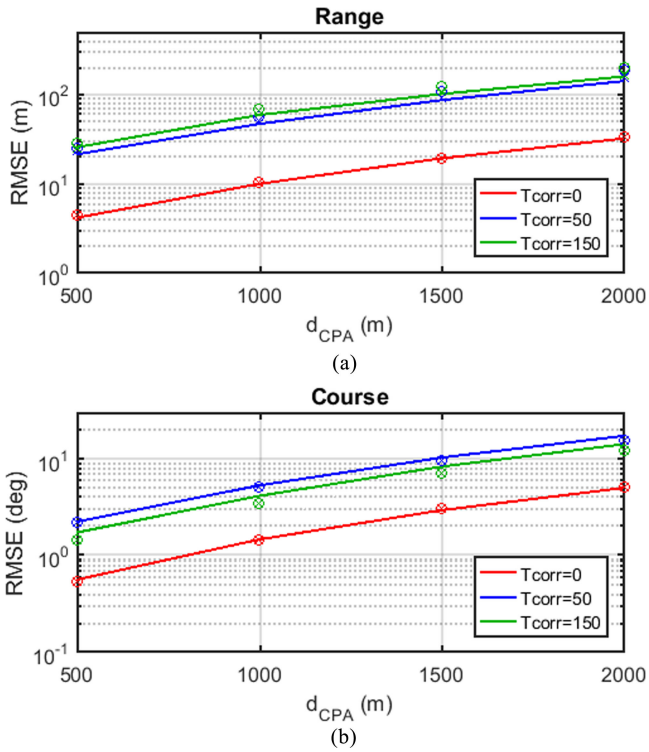

Fig. 1. RMSE of (a) range estimates and (b) heading estimates as functions of CPA distance and correlation interval of bearing errors. Observation time is 200 s; STD of bearing errors is 2°. Cramér–Rao bounds of the estimates (10) were obtained using a diagonal covariance matrix (symbol "○") and a covariance matrix created from linear approximation (symbol "×") (13).

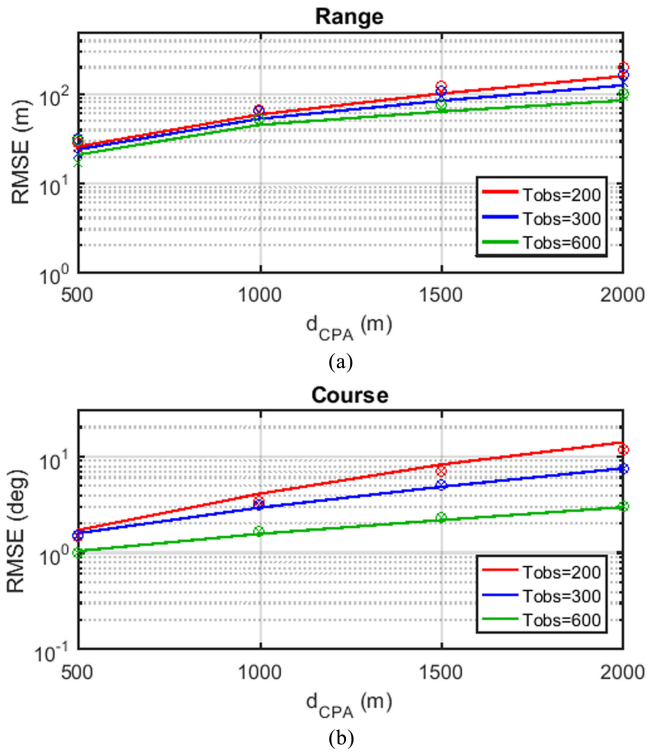

Fig. 2. RMSE of (a) range estimates and (b) heading estimates as functions of CPA distance and observation time. Correlation interval of bearing errors is 150 s; STD of bearing errors is 2°. Cramér–Rao bounds of the estimates (10) were obtained using diagonal covariance matrix (symbol "○") and covariance matrix composed using linear approximation (symbol "×") (13).

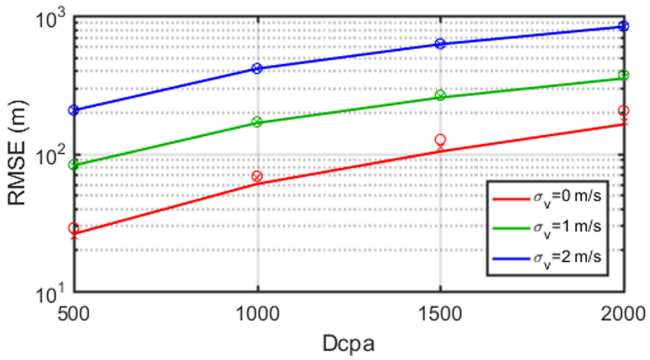

Fig. 3. RMSE of range estimates as functions of CPA distance and STD of speed error. Correlation interval of bearing errors is 150 s; STD of bearing errors is 2°. Cramér–Rao bounds of the estimates (10) were obtained using diagonal covariance matrix (symbol "○") and covariance matrix composed using linear approximation (symbol "×") (13).

obtained for the observation time $T = 200$ s, the correlation interval of bearing errors $\tau_\alpha = 150$ s, and various values of the STD of speed errors σ_v are shown in Fig. 3.

B. In Situ Tests

In situ tests were conducted using a stationary compact tetrahedral array of hydrophones monitored by an Autonomous Multichannel Acoustic Recorder (AMAR, JASCO Applied Sciences) [9]. The array was deployed on the VENUS cabled ocean observatory operated by ONC in the Salish Sea, BC, Canada. Each AMAR had four hydrophones that sampled all four channels at 64 kHz. The sensitivity of the hydrophones and current-to-voltage converter board was −165 dB re 1 V/μPa at 250 Hz. The array was deployed on the seabed at 168-m depth; the hydrophones in the array were approximately 1.84-m apart. The position and orientation of the array was measured during the deployment. The array was calibrated using surface vessels with known GPS coordinates. Although the tetrahedral array used in our tests could measure both azimuth and elevation angles, the parameter estimates (10) were only computed with azimuths.

Typical distribution of speeds, heading angles, and CPA distances of vessels traveling within the distance of 3000 m or less from the array are shown in Fig. 4. These plots were obtained using AIS data transmitted by 3245 vessels. The data were collected from February 17 to March 25 and from June 7 to July 21, 2016. These data were used as the training data set to compute the average speed of vessels in the deployment area. The average speed was $\bar{v} = 7.3\,\mathrm{m/s}$ and its STD was $\sigma_v = 2.3$ m/s.

Vessel azimuths were measured using the ML TDOA-based algorithm [9]

$$\hat{\alpha}(t_k) = \arg\min_{\alpha} \sum_i \sum_j \left(\hat{\tau}_{i,j}(t_k) - \tau_{i,j}(\alpha, \beta_0, d_0)\right)^2 \quad (31)$$

where $\hat{\tau}_{i,j}(t_k)$ is the TDOA estimate between the ith and jth recorder of the array ($i = 1 \ldots 3$, $j = 2 \ldots 4$) computed for the time t_k; $\tau_{i,j}(\alpha, \beta_0, d_0)$ is the expected TDOA computed for the azimuths $\alpha = 0 \ldots 360°$, elevation angle $\beta_0 = 0°$, and range $d_0 = 500$ m. TDOAs of ship noise were computed for

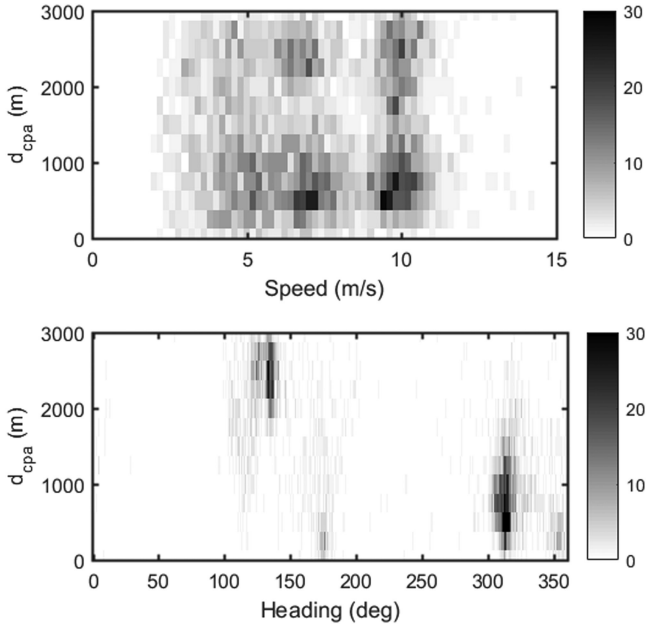

Fig. 4. Two-dimensional distributions of speeds and heading angles versus CPA distances of the 3245 training vessels.

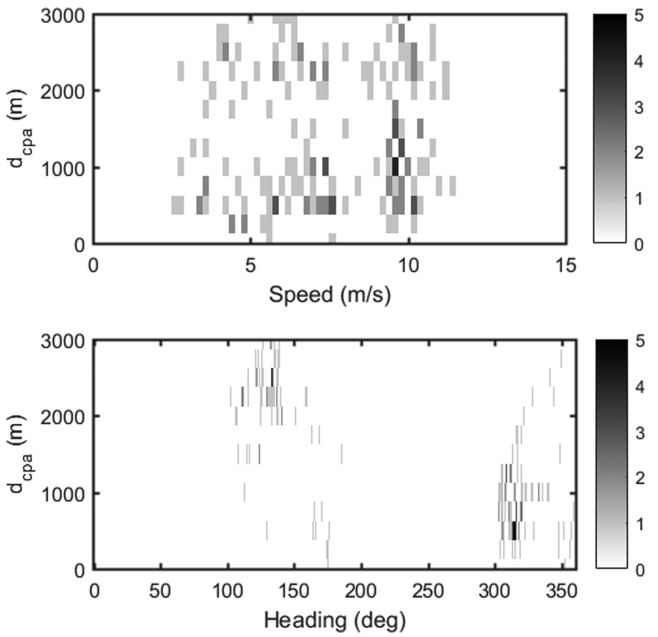

Fig. 5. CPA distances, speeds, and heading angles of the 171 testing vessels.

consecutive 1-s-long data segments each overlapped by 0.5 s in the 50–25 000-Hz frequency range.

We tested the algorithms with data from Feb 21–22, and Aug 17–23, 2016. The tests included 171 vessels with CPA distances of 3000 m or less. The vessels were observed over the interval $t_{\mathrm{CPA}} \pm 100$ s or more. The tests obtained geographic locations and speeds during the passes of these vessels from their AIS broadcasts. The 2-D distribution of speeds, heading angles, and CPA distances of tested vessels are shown in Fig. 5. The average speed of tested vessels was $\bar{v} = 7.5$ m/s and the STD was $\sigma_v = 2.4$ m/s.

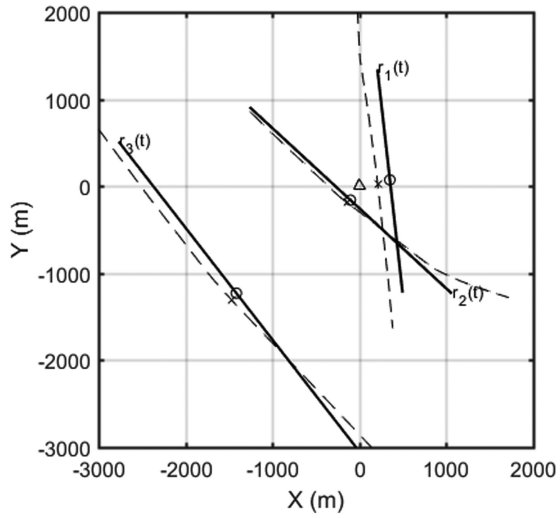

Fig. 6. Vessel positions obtained from AIS data (dashed line) and position estimates (solid lines). Symbols "×" show the CPA positions and symbols "○" display CPA estimates.

As it was stated in Section II, we assumed that the dominant source of vessel noise arises from propulsion systems, and that the acoustic measurements (3), (8) correspond to the average bearing of these components. For large commercial vessels, the average position of these components $\boldsymbol{r}_P(t)$ can differ from the positions broadcast through AIS, which are derived from GPS devices with antennas that can be mounted elsewhere on the vessel, at $\boldsymbol{r}_{\mathrm{GPS}}(t)$. However, both the noise source and the GPS antenna travel in the same trajectory $\boldsymbol{r}_P(t) = \boldsymbol{r}_{\mathrm{GPS}}(t - \tau_P)$, and they will cross the same CPA location with a certain time delay τ_P . Hence, the CPA distance can be found from the GPS coordinates as (30)

$$d_{\mathrm{CPA}} = \min_t |\boldsymbol{r}_P(t) - \boldsymbol{r}_A| = \min_t |\boldsymbol{r}_{\mathrm{GPS}}(t) - \boldsymbol{r}_A| \qquad (32)$$

where $\boldsymbol{r}_A$ is a vector of AIS coordinates of the array center. To improve accuracy, available AIS coordinates were interpolated using the same time grid as that used to estimate azimuths (8), and the interpolated values $\boldsymbol{r}_{\mathrm{GPS}}(t_k),\ k = 1 \ldots K$, were substituted to (32).

All 171 test vessels were divided into seven groups based on their CPA distances, $d_{\mathrm{CPA}} \in \{500,\ 750, \ldots,\ 2000\} \pm 250$ m. The RMSE of the range and heading estimates were computed separately for each group.

Two scenarios were used to test the estimator (10). In the first scenario, the average speed of training vessels, $\bar{v} = 7.3$ m/s was used to compute the ML estimates (10). Fig. 6 shows the trajectories of three vessels, $\boldsymbol{r}_1(t)$, $\boldsymbol{r}_2(t)$, and $\boldsymbol{r}_3(t)$ computed using the AIS coordinates (dashed lines). The CPA distances were $d_{\mathrm{CPA}1} = 212$ m, $d_{\mathrm{CPA}2} = 234$ m, and $d_{\mathrm{CPA}3} = 1967$ m. At the CPA, vessels traveled with the heading angles of $\gamma_1 = 173.6^\circ$, $\gamma_2 = 307.3^\circ$, and $\gamma_3 = 138.2^\circ$ and with the speed of $v_1 = 4.3$ m/s, $v_2 = 10.2$ m/s, and $v_3 = 7.4$ m/s, respectively. The position estimates (11) computed using the average speed $\bar{v} = 7.3$ m/s are shown as a solid line near the corresponding GPS-based trajectories. The RMSE of the range and heading estimates of tested vessels are shown in Fig. 7.

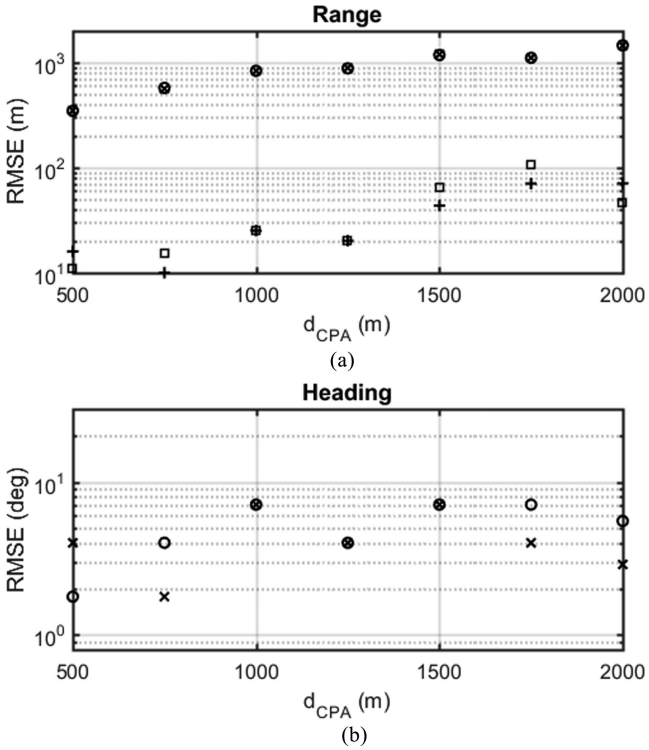

Fig. 7. RMSE of (a) range estimates and (b) heading estimates as functions of CPA distance obtained in *in situ* tests. Parameter estimates (10) were obtained for the average vessel speed of 7.3 m/s (scenario 1) using a diagonal covariance matrix (symbol "×") and a nondiagonal covariance matrix (symbol "○"). Range estimates obtained for the actual speed of vessels (scenario 2) are shown by the symbols "+" (diagonal covariance matrix) and "□" (nondiagonal covariance matrix).

In the second scenario, the parameter estimates (10) were computed for each vessel using its CPA speed, which was obtained from the AIS data. Although this scenario is impractical, the results of this test represent the potential accuracy provided by the bearing-only ML estimator (10) when the source speed is known. Since heading errors do not depend on speed errors, the RMSE of heading estimates observed in scenario 2 are similar to those in scenario 1. The RMSE of the range estimates are shown in Fig. 7(a).

V. Discussion and Conclusion

The main difficulty in implementing the ML estimator (10) when correlated bearing errors are present, was that the invertible matrix could approximate the covariance matrix of correlated bearing errors $\boldsymbol{C}$. Among the models (12)–(14), using a linear model (13) provides the best tradeoff between the singularity property and approximation accuracy. Comparing the estimators (10) using a diagonal covariance matrix and the matrix with nonzero off-diagonal elements showed that estimation accuracy decreases if correlation properties of bearing errors are ignored, albeit only a small amount compared to other factors that affected performance.

Statistical simulations revealed that significant factors affecting the accuracy of the range and heading estimates are CPA distance d_{CPA}; correlation interval of bearing errors τ_α; and

observation time T. Speed errors increase the RMSE of the range estimates and do not affect the heading estimation accuracy. Both statistical simulations (see Fig. 3) and *in situ* tests (Figs. 6 and 7) show that speed errors affected the range estimation accuracy more than any other factor. Simulations show that if the STD of speed errors is higher than 1 m/s, the influence of other factors becomes negligibly small. This means that stationary compact arrays using bearing only measurements can be inefficient for accurately estimating positions of sources whose speeds differ from the expected value. A possible method of mitigating this issue is to use other means, such as shaft rate calculations made using the raw acoustic data, to improve the speed estimate. The speed error problem can also be avoided if the compact array is deployed at a depth comparable with the distance to vessel such that both azimuth and elevation measurements can be used for direct estimation of vessel ranges. However, this situation is not considered in this work.

Using stationary compact arrays can be extremely beneficial to many applications associated with long-term PAM of vessels and marine mammals over large areas. In addition to the standard tasks of detecting signals and classifying sources, stationary compact arrays make it possible to count the number of sources transiting a surveillance area, and to accurately estimate their heading angles, which indicate the direction they are traveling. The accuracy of position and range estimates strongly depends on the source speed variation and thus might not be useful for sources whose speeds cannot be estimated accurately.

The results of statistical simulations demonstrate that in the case of Gaussian bearing errors and in the absence of speed errors, the RMSE of the range, and heading ML estimates (10) are close to the CRB (see Figs. 1 and 2). If there are speed errors, the corresponding RMSE are represented by (20) (see Figs. 3 and 7).

Thus, stationary compact arrays can be considered as an efficient tool for various PAM applications. They provide many benefits compared to the stationary omnidirectional sensors and large arrays of synchronized sensors. The results from this work make it possible to implement the ML position and heading angle estimators in compact arrays and to evaluate their performance before the array is deployed. However, this work has omitted two important issues: estimating motion parameters of sources that move at variable speed and heading angles, and BO-TMA using multiple stationary compact arrays, which should be researched further.

ACKNOWLEDGMENT

The authors would like to thank the JASCO field team for deploying the compact array and K. Williams and K. Hiltz for help editing the draft version of the manuscript.

REFERENCES

[1] I. R. Urazghildiiev and C. W. Clark, "Comparative analysis of localization algorithms with application to passive acoustic monitoring," *J. Acoust. Soc. Amer.*, vol. 134, no. 6, pp. 4418–4426, Jan. 2010.

[2] K. W. Chung, A. Sutin, A. Sedunov, and M. Bruno, "DEMON acoustic ship signature measurements in an Urban harbor," *Adv. Acoust. Vib.*, vol. 2011, pp. 1–13, 2011.

[3] A. Tesei, S. Fioravanti, V. Grandi, P. Guerrini, and A. Maguer, "Localization of small surface vessels through acoustic data fusion of two tetrahedral arrays of hydrophones," in *Proc. 11th Eur. Conf. Underwater Acoust.*, Jul. 2012, pp. 1–12.

[4] R. Hirotsu *et al.*, "Localization of sperm whales in a group using clicks received at two separated short baseline arrays," *J. Acoust. Soc. Amer.*, vol. 127, no. 1, pp. 133–147, Jan. 2010.

[5] S. M. Wiggins, M. A. McDonald, and J. A. Hildebrand, "Beaked whale and dolphin tracking using a multichannel autonomous acoustic recorder," *J. Acoust. Soc. Amer.*, vol. 131, no. 1, pp. 156–163, Jan. 2012.

[6] S. M. Wiggins, K. E. Frasier, E. E. Henderson, and J. A. Hildebrand, "Tracking dolphin whistles using an autonomous acoustic recorder array," *J. Acoust. Soc. Amer.*, vol. 133, no. 6, pp. 3813–3818, Jun. 2013.

[7] M. Gassmann, E. E. Henderson, S. M. Wiggins, M. Roch, and J. A. Hildebrand, "Offshore killer whale tracking using multiple hydrophone arrays," *J. Acoust. Soc. Amer.*, vol. 134, no. 5, pp. 3513–3521, Nov. 2013.

[8] M. Gassmann, S. M. Wiggins, and J. A. Hildebrand, "Three-dimensional tracking of Cuvier's beaked whales' echolocation sounds using nested hydrophone arrays," *J. Acoust. Soc. Amer.*, vol. 138, no. 4, pp. 2483–2494, Oct. 2015.

[9] I. R. Urazghildiiev and D. Hannay, "Maximum likelihood estimators and Cramér–Rao bound for localization using compact arrays," *J. Acoust. Soc. Amer.*, vol. 141, no. 4, pp. 2548–2555, Apr. 2017.

[10] S. C. Nardone and V. G. Aidala, "Observability criteria for bearing-only target motion analysis," *IEEE Trans. Aerosp. Electron. Syst.*, vol. 17, no. 2, pp. 162–166, Mar. 1981.

[11] S. C. Nardone, A. G. Lingren, and K. F. Gong, "Fundamental properties and performance of conventional bearing-only target motion analysis," *IEEE Trans. Autom. Control*, vol. 29, no. 9, pp. 775–787, Sep. 1984.

[12] S. C. Nardone and M. L. Graham, "A closed form solution to bearing-only target motion analysis," *IEEE J. Ocean. Eng.*, vol. 22, no. 1, pp. 168–178, Jan. 1997.

[13] K. Becker, "Target motion analysis," in *Advanced Signal Processing Handbook: Theory and Implementation for Radar, Sonar, and Medical Imaging Real-Time Systems*. Boca Raton, FL, USA: CRC Press, 2001, ch. 9, pp. 372–392.

[14] Y. Bar-Shalom, X. R. Li, and T. Kirubarajan, *Estimation With Applications to Tracking and Navigation*, New York, NY, USA: Willey, 2001, ch. 3, pp. 161–171.

[15] D. Musicki, "Bearing only single-sensor tracking using Gaussiam mixtures," *Automatica*, vol. 45, pp. 2088–2092, Jun. 2009.

[16] R. Radhakrishnan, A. K. Singh, S. Bhaumik, and N. K. Tomar, "Quadrature filters for underwater passive bearings-only target tracking," *Presented at Sensor Signal Process. Def.*, Edinburgh, Scotland, 2015. [Online]. Available: ieeexplore.ieee.org/iel7/7287474/7288486/07288519.pdf

[17] C. Jauffret, D. Pillon, and A.-C. Pignol, "Bearings-only TMA without observer maneuver," in *Proc. 11th Int. Conf. Inf. Fusion*, 2008. [Online].Available: http://ieeexplore.ieee.org/document/4632252/

[18] F. Bavencoff, J.-M. Vanpeperstraette, and J.-P. Le Cadre, "Constrained bearings-only target motion analysis via Markov chain Monte Carlo methods," *IEEE Trans. Aerosp. Electron. Syst.*, vol. 42, no. 4, pp. 1240–1263, Oct. 2006.

[19] Y. J. Zhang and G. Z. Xu, "Bearings-only target motion analysis via instrumental variable estimation," *IEEE Trans. Signal Process.*, vol. 58, no. 11, pp. 5523–5533, Nov. 2010.

[20] L. Bardisal and K. Dogancay, "Three-dimensional target motion analysis using azimuth/elevation angles," *IEEE Trans. Aerosp. Electron. Syst.*, vol. 50, no. 4, pp. 3178–3194, Oct. 2014.

[21] K. Dogancay, "3D pseudolinear target motion analysis from angle measurements," *IEEE Trans. Signal Process.*, vol. 63, no. 6, pp. 1570–1580, Mar. 2015.

[22] F. Dommermuth and J. Schiller, "Estimating the trajectory of an accelerationless aircraft by means of a stationary acoustic sensor," *J. Acoust. Soc. Amer.*, vol. 76, no. 4, pp. 1114–1122, Oct. 1984.

[23] K. W. Lo and B. G. Ferguson, "Broadband passive acoustic technique for target motion parameter estimation," *IEEE Trans. Aerosp. Electron. Syst.*, vol. 36, no. 1, pp. 163–175, Jan. 2000.

[24] A. Pollara, A. Sutin, and H. Salloum, "Modulation of high frequency noise by engine tones of small boats," *J. Acoust. Soc. Amer.*, vol. 142, no. 1, pp. EL30–EL34, Jul. 2017.

[25] S. M. Kay, *Fundamentals of Statistical Signal Processing: Estimation Theory*. Upper Saddle River, NJ, USA: Prentice-Hall, 1998, ch. 3, pp. 27–53.

Ildar R. Urazghildiiev received the M.Sc. degree from the Zhitomir Institute of Radioelectronics, Zhitomir, Ukraine, in 1989 and the Ph.D. degree from the National R&D Center of Defense Technologies and Military Security of Ukraine, Kiev, Ukraine, in 1996, both in electrical engineering.

From 1994 to 2001, he was with the National R&D Center of Defense Technologies and Military Security of Ukraine and the National Technical University of Ukraine "Kiev Polytechnic Institute," Kiev, Ukraine. In 2001 and 2003, he held a Postdoctoral Fellow position at the Signals and Systems Group, Uppsala University, Uppsala, Sweden. From 2004 to 2014, he was a Research Associate at the Lab of Ornithology, Cornell University, Ithaca, NY, USA. In 2014, he joined JASCO Applied Sciences, Inc., Anchorage, AK, USA, where he is currently a Senior Research Engineer. His research interests include statistical signal processing, signal detection, parameter estimation, classification, localization, and tracking with applications to bioacoustics.

David E. Hannay received the B.Sc. and M.Sc. degrees in physics from the University of Victoria, BC, Canada, in 1988 and 1994, respectively.

Since 1989, he has been a Research Scientist at JASCO Applied Sciences, Inc., Victoria, BC, Canada, specializing in underwater acoustic modeling for environmental noise assessments. He is presently the Chief Science Officer for JASCO's multinational science teams. He develops computer models for predicting acoustic pressure and particle velocity, and applies those to a variety of industrial noise sources including sonars, explosives, aircraft, seismic exploration sources, shipping, and pile driving. His recent work is related to ship noise measurements and quieting technologies.